Effect of water content on permanent deformation of fine/coarse soil mixtures with varying coarse grain contents and subjected to multi-stage cyclic loading

Yu Su, Yu-Jun Cui, Jean-Claude Dupla, Jean Canou

Effect of water content on permanent deformation of fine/coarse soil mixtures with varying coarse grain contents and subjected to multi-stage cyclic loading

Yu Su[1,2], Yu-Jun Cui[2], Jean-Claude Dupla[2], Jean Canou[2]

1: School of Civil Engineering and Architecture, Nanchang University, Nanchang 330031, China

2: Laboratoire Navier/CERMES, Ecole des Ponts ParisTech (ENPC), France

Corresponding author

Yu SU

1. School of Civil Engineering and Architecture, Nanchang University, Nanchang 330031, China

2. Ecole des Ponts ParisTech, Laboratoire Navier/CERMES, 6 – 8 av. Blaise Pascal, Cité Descartes, Champs-sur-Marne, 77455 Marne – la – Vallée cedex 2, France

E-mail address: yu.su@enpc.fr

Abstract

An interlayer soil in ancient rail tracks was identified as a mixture of ballast grains and subgrade fines. As the permanent strain ε_1^p of such mixture was affected by water content, cyclic triaxial tests were performed, under varying water contents of fines w_f and coarse grain contents f_v. Comparison between present and previous studies showed the significant effect of sample preparation method on ε_1^p. In present study, a constant fine dry density $\rho_{d\text{-}f}$ was maintained, leading to an unchanged suction of mixture whatever the f_v value. In this case, only the reinforcement effect of f_v on ε_1^p was identified. By contrast, in previous studies, the global dry density of mixture ρ_d was kept constant, resulting in a decrease of $\rho_{d\text{-}f}$ with increasing f_v and consequently a decrease of suction. In this case, when the negative effect of decreasing suction prevailed on the positive reinforcement effect of increasing f_v, the ε_1^p increased.

Keywords: interlayer soil; cyclic triaxial test; permanent deformation; water content; coarse grain content; fabric/ structure of soils

INTRODUCTION

An interlayer was created in most conventional French rail tracks, mainly due to the interpenetration of ballast grains and subgrade fine soils. This interlayer was maintained in the railway substructure in the French program of rail track renewal considering its high dry density (2.4 Mg/m^3, Trinh [1]), Cui et al. [2]) and, hence, bearing capacity. As an important component of rail track, the interlayer soil diffused static and dynamic stresses into the substructure, avoiding excessive deformation. In this case, the deformation behavior of interlayer soil appeared to be significant, especially for the long-term stability of rail track. Field observation showed that the ballast grain content decreased over depth in the interlayer soil (Trinh [1]). However, the interlayer could be approximately divided into two parts: the upper part dominated by ballast grains and the lower part dominated by subgrade fine soil. With the unstable groundwater and climate change (rainfall and evaporation), the water content of interlayer soil can change over time, significantly affecting its permanent deformation behavior. Thus, in order to ensure the good serviceability of the tracks, it is essential to understand the effect of water content on the permanent deformation of interlayer soil.

The effect of coarse grain content on permanent deformation of soil have been investigated by several investigators. Song and Ooi [3] studied the deformation behaviour of aggregates with varying fine soil contents, and found that increasing fine content gave rise to an increase of permanent deformation of soil mixtures. Wang et al. [4] investigated the effect of coarse grain content f_v (ratio of coarse grain volume to total volume) on permanent strain of interlayer soil by cyclic triaxial tests. They identified a characteristic coarse grain content $f_{v\text{-}cha}$

in a narrow range from 25.8% to 27.8%: a large decrease of permanent strain with f_v was observed at $f_v \leq f_{v\text{-}cha}$, but a slight decrease of that at $f_v \geq f_{v\text{-}cha}$. It is worth noting that these tests were performed under a constant water content of fine soils fraction $w_{opt\text{-}f} = 13.7\%$, and the effect of water content was not specifically addressed . Some studies evidenced the effect of water content on permanent deformation of substructures: at saturation, an excess pore water pressure accumulated under traffic loadings led to a decrease of effective stress and an increase of permanent deformation. When the water content decreased, the permanent deformation appeared to decrease, which was attributed to the contribution of suction (Gidel et al. [5]; Werkmeister et al. [6]; Nie et al. [7]; Trinh et al. [8]; Jing [9]; Wan et al. [10]). Gu et al. [11] studied the permanent deformation of unbound granular materials by suction-controlled cyclic triaxial tests, and reported that an increase of suction led to a decrease of accumulated permanent strain exponentially under varying deviator stress amplitudes. Duong et al. [12] investigated the effect of water content on permanent deformation of the upper interlayer soil with varying fine soil contents, and found that the effects of water content and fine content on permanent deformation were strongly related. At saturated state, an increase of fine content gave rise to an increase of permanent deformation, while at unsaturated state, an opposite trend was observed, due to the contribution of suction developed in the fines. Jing [9] studied the deformation behaviour of granular material with varying water contents and fine contents, and also reported that increasing fine content led to an increase of permanent deformation under saturated condition and a decrease of that under unsaturated condition. Note that in most studies, the dry density of fine/coarse soil mixtures remained constant during the sample preparation; thereby a variation of dry density of fine soil fraction was

induced with varying fine contents (or coarse grain contents). In that case, both suction and coarse grain content varied, rendering the test results difficult to be analysed.

This study aims at investigating the effect of water content on the permanent deformation of fine/coarse soil mixtures under various coarse grain contents. A series of cyclic triaxial tests were performed for this purpose. Emphasis was put on keeping the fine dry density $\rho_{d\text{-}f}$ constant in all samples, allowing a constant suction of soil mixtures whatever the f_v value. A multi-step loading procedure at various deviator stress amplitudes of 10, 15, 20, 25 and 30 kPa was applied, with a number of loading cycles at 90000 for each stress amplitude. Two target water contents of fine soil (17.6% and 10.6%) and five coarse grain contents (0%, 10%, 20%, 35% and 45%) were considered.

MATERIALS AND SAMPLE PREPARATION

Considering the difficulty of obtaining intact interlayer soil from the field, the reconstituted soils consisting of fine soil and coarse grains were fabricated in the laboratory. For re-constituting the fine soil, nine different commercial soils (Table 1) are mixed with the pre-determined proportions, to obtain a similar grain size distribution curve of fines from 'Senissiat site' (Fig. 1). Note that in this study fines refer to the soil finer than ballast in the field, which correspond to a mixture encompassing grains of clay to sand sizes. The liquid limit and plasticity index of reconstituted fine soil were 32% and 20%, respectively, classifying the soil as CL based on the universal soil classification system. Fig. 2 presents the standard proctor compaction curve of fine soil, defining an optimum water content $w_{opt\text{-}f}$ = 13.7% and a maximum dry density $\rho_{dmax\text{-}f}$ = 1.82 Mg/m^3.

For the coarse grains, based on a parallel gradation method applied by Wang et al. [13] , Qi et al. [14] and Su et al. [15-17] , which was verified later by Qi et al. [18] , micro-ballast was adopted to replace the real ballast in Fig.1. A parameter of coarse grain content f_v (Wang et al. [13]), defined as the ratio of the volume of coarse grains V_c to the total volume of fine/coarse mixture V (Eq. (1)), was adopted in this study. All voids and water were assumed to be contained in the fine soil (Fig. 3). Thus, under a given f_v, the dry density of fine soil $\rho_{d\text{-}f}$ and the water content of fine soil w_f, the masses of coarse grain $m_{s\text{-}c}$, fine grain $m_{s\text{-}c}$ and the water content of fine soil $m_{w\text{-}f}$ were calculated by Eqs. (2) – (4), respectively.

$$f_v = \frac{V_c}{V} = \frac{V_c}{V_c+V_f} = \frac{V_c}{V_c+V_{s-f}+V_{w-f}+V_{a-f}} \quad (1)$$

where V_f is the volume of fine soil; $V_{s\text{-}f}$, $V_{w\text{-}f}$ and $V_{a\text{-}f}$ are the volume of fine grains, water and air in the fine soil, respectively.

$$m_{s-c} = V_c \cdot G_{s-c} \cdot \rho_w = f_v \cdot V \cdot G_{s-c} \cdot \rho_w \quad (2)$$

$$m_{s-f} = \rho_{d-f} \cdot V_f = \rho_{d-f} \cdot V \cdot (1 - f_v) \quad (3)$$

$$m_{w-f} = w_f \cdot m_{s-f} \quad (4)$$

where $G_{s\text{-}c}$ is the specific gravity of coarse grains (= 2.68 Mg/m^3); ρ_w is the water unit mass.

Table 1. Nine different commercial soils

Soil classification	Commercial Soil	Mass proportion (%)	The range of grain size (mm)
Sand	HN34	3.3	0.063 - 0.50
	HN31	3.3	0.16 - 0.63

	HN0.4-0.8	6.7	0.25 - 1
	HN0.6-1.6	6.7	0.32 - 2
	HN1-2.5	13.3	0.32 – 3.20
	C4	16.7	0.0009 – 0.50
	C10	20	0.0009 – 0.25
Clay	Speswhite	23.3	0.0003 – 0.01
	Bentonite	6.7	0.001 – 0.01

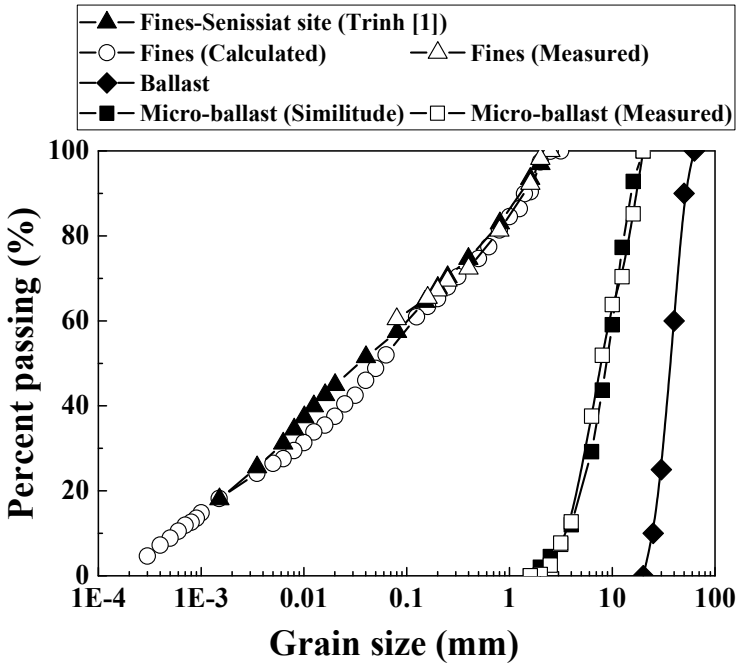

122 Fig. 1. Grain size distribution curves of fine soil and micro-ballast (after Wang et al. [4])

123

124

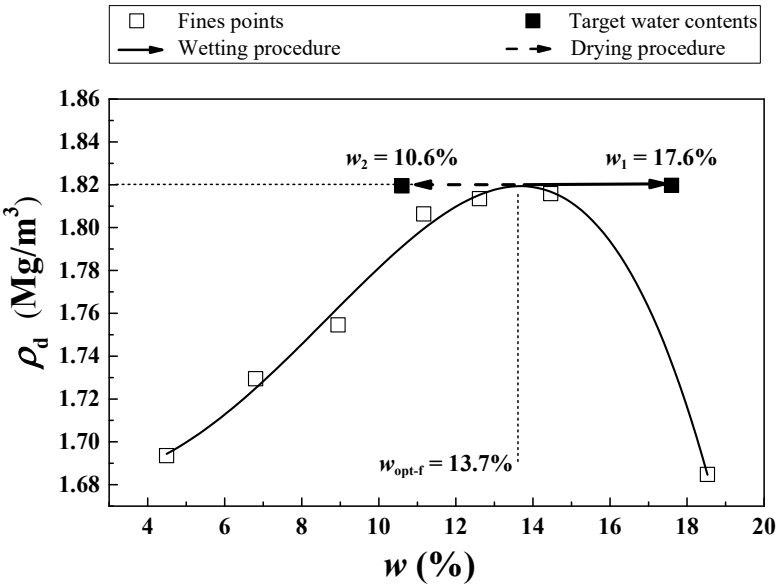

Fig. 2. Preparation of samples at two target water contents with respect to compaction curve of the fine soil

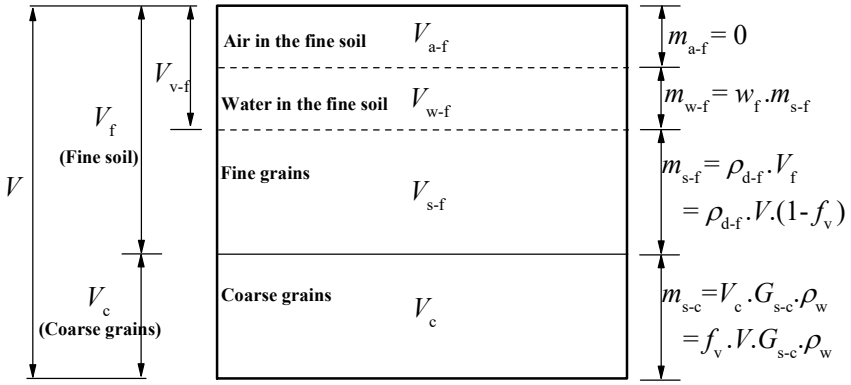

Fig. 3. Constitution of fine/coarse soil mixture

In order to prepare a sample at a target f_v value and a target water content w_f, the fine soil was prepared at w_{opt-f} = 13.7%, then stored in a container for 24h for the purpose of moisture homogenization. After that, the fine soil was mixed with coarse grains at the pre-determined mass to reach the target f_v value. The soil mixture was then dynamically compacted in three layers, with the equivalent amounts of fine soil and coarse grains for each layer, to attain a

size of 100 mm diameter and 200 mm height. Note that the fine soil was kept at the maximum dry density $\rho_{dmax\text{-}f}$ = 1.82 Mg/m^3 for all samples with varying f_v values. With a higher f_v value, more compaction energy was needed for the soil mixtures; thereby, a higher dry density ρ_d of sample is obtained (Table 2). It is worth noting that when $f_v > f_{v\text{-}cha}$, the coarse grains constitute the skeleton of soil mixture (Wang et al. [4]). For this fabric, two categories of fine soil were identified by Su et al. [19] – dense fine soil between coarse grains and loose fine soil surrounded by coarse grains. Accordingly, a relative high $\rho_{d\text{-}f}$ and low $\rho_{d\text{-}f}$ was obtained for dense fines and loose fines, respectively, even though the global $\rho_{d\text{-}f}$ of fine soil remained constant (1.82 Mg/m^3).

After compacting a sample at a target f_v value, either a wetting or a drying process was adopted for the sample to reach the target water contents w_f (Fig. 2): w_1 = 17.6% (S_r = 100%) on the wet side and w_2 = 10.6% (S_r = 60%) on the dry side. The approach of wetting or drying from $w_{opt\text{-}f}$ = 13.7% to the target w_f value proposed by Su et al. [19] was applied: in the case of drying, the sample was each time exposed to the air for 1 h in the laboratory, and then covered with plastic film for at least 7 h equilibration. In the case of wetting, 10 g water was sprayed on the sample each time, and then wrapped it with plastic film and conserved for the same equilibration time of at least 7 h.

During the wetting and drying processes, the volume change of samples under different f_v values was recorded (Fig. 4). It can be observed that at a given f_v value, the swelling of sample upon wetting from $w_{opt\text{-}f}$ = 13.7% to w_1 = 17.6% or shrinkage of that upon drying from $w_{opt\text{-}f}$ = 13.7% to w_2 = 10.6% occurred. Moreover, the magnitude of swelling-shrinkage of sample decreased with the increase of f_v, which was attributed to (*i*) a reduction of fine soil, which

was sensitive to water content change and (*ii*) part of total stress supported by the coarse grain skeleton at $f_v > f_{v\text{-}cha}$ (Wang et al. [4]). This response of fine/coarse soil mixture appeared to be dominated by the fine matrix for $f_v < 20\%$ but the coarse grain skeleton for $f_v > 35\%$ (Fig. 4).

The measured dry density ρ_d of sample after wetting or drying is shown in Table 2.

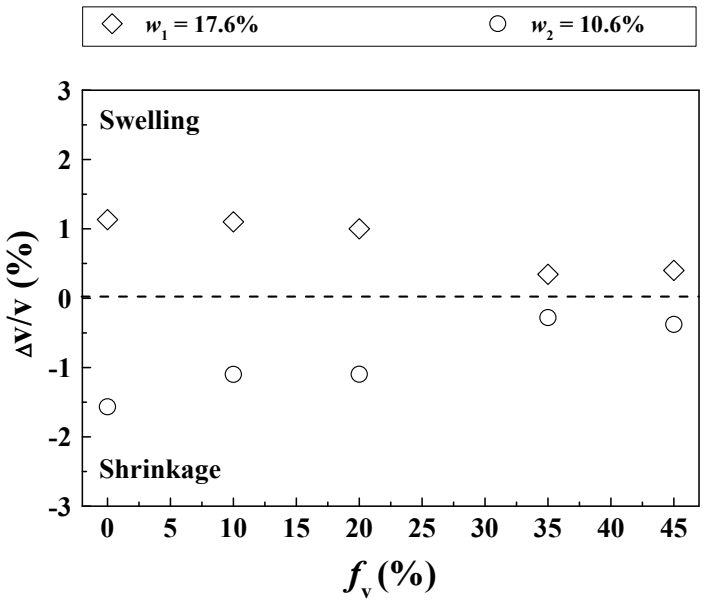

Fig. 4. Variations of sample volume with f_v at two target water contents

Table 2. Experimental program of cyclic triaxial tests

f_v (%)	Initial water content $w_{opt\text{-}f}$ (%)	Target w_f (%)	Target S_r (%)	Target $\rho_{dmax\text{-}f}$ (Mg/m^3)	Target ρ_d (Mg/m^3)	Measured ρ_d (Mg/m^3)
0	13.7	17.6	100	1.82	1.82	1.80
		10.6	60			1.85
10		17.6	100		1.91	1.88
		10.6	60			1.93
20		17.6	100		1.99	1.97
		10.6	60			2.01
35		17.6	100		2.12	2.11
		10.6	60			2.13
45		17.6	100		2.21	2.20
		10.6	60			2.22

Note: f_v represents the volumetric ratio of coarse grains to fine/coarse soil mixtures. $w_{opt\text{-}f}$, w_f, S_r and $\rho_{dmax\text{-}f}$ represent the optimum water content, water content, degree of saturation and maximum dry density of fine soil, respectively. ρ_d represents the dry density of soil mixtures sample. Measured ρ_d represents the dry density of soil mixtures sample after wetting or drying from compaction water content $w_{opt\text{-}f}$ to target w_f.

CYCLIC TRIAXIAL TESTS

The cyclic triaxial apparatus used by Wang et al. [20] was adopted in this study, hosting a sample with 100 mm diameter and 200 mm height. Using a 50 kN hydraulic actuator enabled a force or displacement controlled mode to be applied in both monotonic and cyclic triaxial tests. As for the cyclic loading, different signal shapes, amplitudes, frequencies and large number of cycles (up to several millions) can be applied. A linear variable displacement transducer (LVDT) was adopted to monitor the axial displacement, with a minimum capacity of ± 0.1mm. Considering the height (= 200mm) of the sample, the corresponding minimum measurement capacity of axial strain was ± 0.05%. A force sensor installed at the bottom was adopted to monitor the axial force.

A series of cyclic triaxial tests were performed on the samples at two target w_f values (w_1 = 17.6% and w_2 = 10.6%) and five f_v values (0%, 10%, 20%, 35% and 45%) with drainage valves open to air. A constant confining pressure σ_3 = 30 kPa was applied, corresponding to the estimated average horizontal stress in the field by the consideration of train loadings, the depth of interlayer soil and the Poisson's ratio (Duong et al. [21]). In the case of w_1 = 17.6% (S_r = 100%), after applying the confining pressure σ_3 = 30 kPa, an overnight consolidation of

179 the sample was adopted, with both the top and bottom porous disks exposed to the air. This
180 allowed for the fully dissipation of generated pore water pressure. On the contrary, in the case
181 of w_2 = 10.6% (S_r = 60%), after application of the confining pressure σ_3 = 30 kPa, the cyclic
182 loading was directly applied, because only air was expected to be expelled.

183 Fig. 5 shows a sine-shaped signal applied at a frequency of 1.78 Hz, corresponding to that
184 excited by two bogies at a train speed of 50 km/h. A multi-step loading procedure proposed by
185 Gidel et al. [5] , applied later by Wang et al. [4] was adopted, which can not only reduce the
186 number of tests but also avoid experimental dispersion due to the variability of sample. Fig. 6
187 depicts a multi-step loading procedure with various deviator stress amplitudes Δq of 10, 15, 20,
188 25 and 30 kPa, and a number of loading cycles N = 90000 for each Δq value. The deviator
189 stress amplitude Δq was defined as the difference of maximum deviator stress q_{max} and
190 minimum deviator stress q_{min}. These Δq values corresponded to the vertical stresses at varying
191 depths of interlayer soil in the field, as reported by Lamas-Lopez [22]. The number of loading
192 cycles N = 90000 was considered large enough for the stabilization of permanent strain under
193 a given Δq value, according to the number applied in previous studies (Gidel et al. [5]; Trinh
194 et al. [8]; Duong et al. [12]; Lamas-Lopez et al. [22]). Note that a constant cyclic stress ratio
195 $\Delta q/\Delta p$ = 3 was adopted, which represented the typical stress path in the interlayer (Trinh et al.
196 [8]). During the tests, the deviator stress and axial strain were recorded.
197

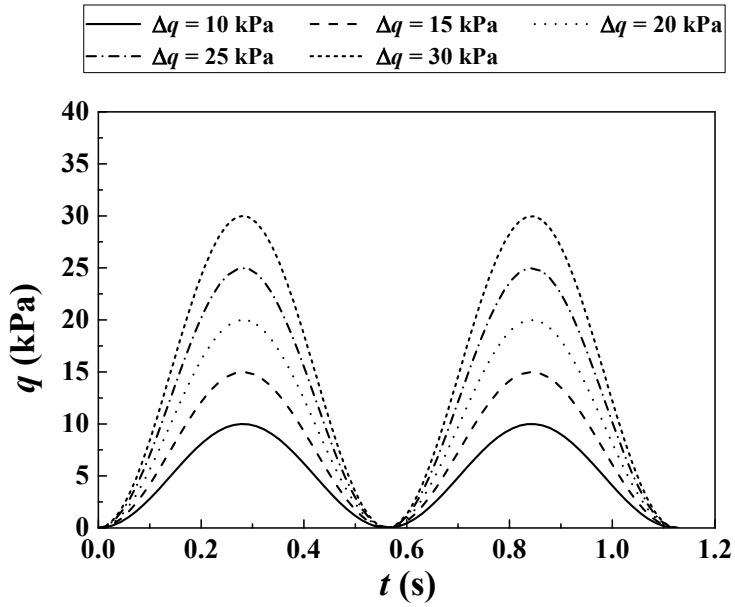

Fig. 5. Typical sine-shaped signals applied in cyclic triaxial tests

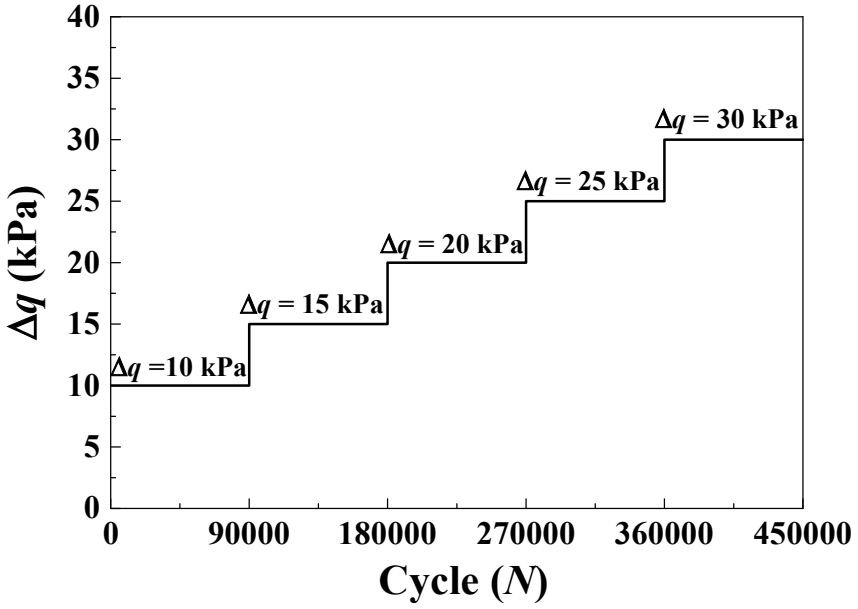

Fig. 6. Multi-step loading procedure with various stress amplitudes Δq

198

199 RESULTS AND DISCUSSIONS

200 *Effect of water content on the evolution of permanent strain with loading cycles*

Fig.7 depicts the evolution of axial strain ε_1 with loading cycles N at f_v = 0% and w_1= 17.6% under various Δq values ranging from 10 kPa to 30 kPa. It can be observed that under a given Δq value, the axial strain ε_1 increased significantly at the beginning of loading cycles, and then gradually stabilized. With the increase of Δq, the axial strain ε_1 increased significantly. In addition, the axial strain ε_1 could be separated into two parts: a plastic strain ε_1^p and a resilient strain ε_1^r. For the plastic strain ε_1^p, it increased with N and the increasing rate decreased with N under a constant Δq value. On the contrary, the resilient strain ε_1^r remained almost unchanged at a given Δq value and increased with increasing Δq.

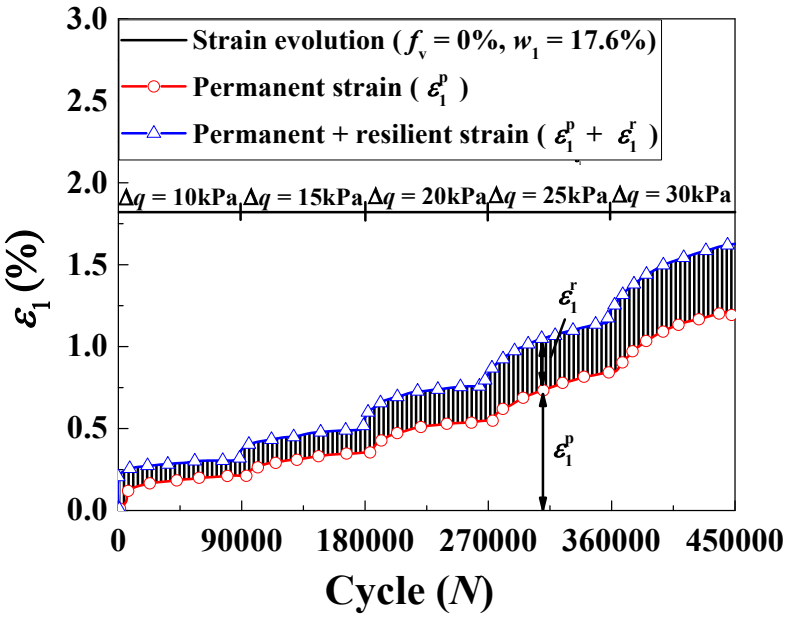

Fig. 7. Determination of permanent strain and resilient strain

Fig. 8 presents the evolutions of ε_1^p with N under various Δq values for f_v = 0% and three water contents. At w_1 = 17.6% , the permanent strain ε_1^p increased with N sharply at the initial loading cycles N, and then gradually reached stabilization under a specific Δq value. With the

increase of Δq, the permanent strain ε_1^p growed significantly. The similar observation can be made in the case of $w_{\text{opt-f}}$ = 13.7% (obtained by Wang et al. [4]) and w_2 = 10.6%. In addition, it can be observed that the decrease of water content from w_1 = 17.6% to $w_{\text{opt-f}}$ = 13.7% or w_2 = 10.6% led to a pronounced decrease of ε_1^p. This could be explained by the contribution of suction, as reported by Duong et al. [12-] and Jing [24].

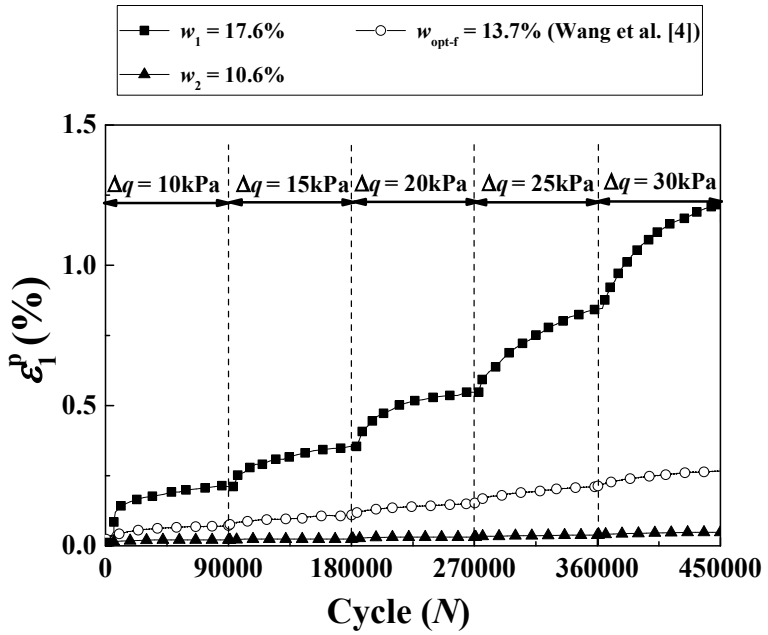

Fig. 8. Evolutions of permanent strain with number of cycles at f_v = 0% and different Δq values for three different water contents

Fig. 9 shows the effect of water content on the evolutions of ε_1^p with N under various f_v values. In the case of w_1 = 17.6% (Fig. 9 (a)), under a given f_v value, the increasing trend of ε_1^p versus N decreased with the increase of N at a constant Δq value. However, ε_1^p increased significantly with the increase of Δq. In addition, it can be found that with the increase of f_v, the permanent strain ε_1^p decreased. This was attributed to the reinforcement effect of coarse

grains in the soil mixtures. Moreover, different decreasing trends of ε_1^p with f_v was evidenced at $f_v \leq 20\%$ and $f_v \geq 35\%$: a pronounced decrease of ε_1^p with f_v at $f_v \leq 20\%$ and a slight decrease of that at $f_v \geq 35\%$. This could be explained by the transition of two soil fabrics: a fine soil dominated fabric at $f_v \leq 20\%$ and a coarse grain dominated fabric at $f_v \geq 35\%$. Note that for the coarse grain skeleton fabric (f_v >35), two categories of fine soil were identified by Su et al. [19] – dense fines (with $\rho_{d\text{-}f}$ higher than 1.82 Mg/m^3) and loose fines (with $\rho_{d\text{-}f}$ lower than 1.82 Mg/m^3). In spite of this inhomogeneous distribution of fine soil in the mixture, the suction of mixture was found to be mainly controlled by the global dry density of fines $\rho_{d\text{-}f}$ = 1.82 Mg/m^3 (Su et al. [25]). The similar observation was made at $w_{opt\text{-}f}$ = 13.7% (Fig. 9 (b)), which was obtained by Wang et al. [4]. At w_2 = 10.6% (Fig. 9 (c)), the ε_1^p at f_v = 0% was very small, with a maximum value around 0.05% identified. The ε_1^p at f_v = 10%, 20%, 35% and 45% was expected to be smaller than that at f_v = 0%. Considering the minimum measurement capacity (0.05%) of axial strain by the adopted LVDT, inaccuracy measurements of ε_1^p at f_v = 10%, 20%, 35% and 45% were generated. Therefore, these results are not presented in Fig. 9 (c).

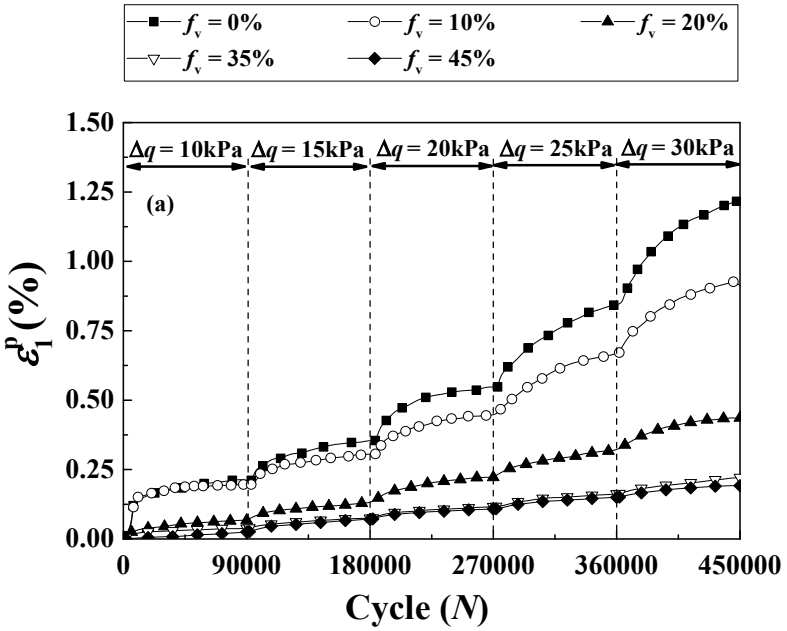
f_v = 0%
f_v = 10%
f_v = 20%
f_v = 35%
f_v = 45%
Δq = 10kPa
Δq = 15kPa
Δq = 20kPa
Δq = 25kPa
Δq = 30kPa
(a)
ε_1^p(%)
1.50
1.25
1.00
0.75
0.50
0.25
0.00
0
90000
180000
270000
360000
450000
Cycle (N)

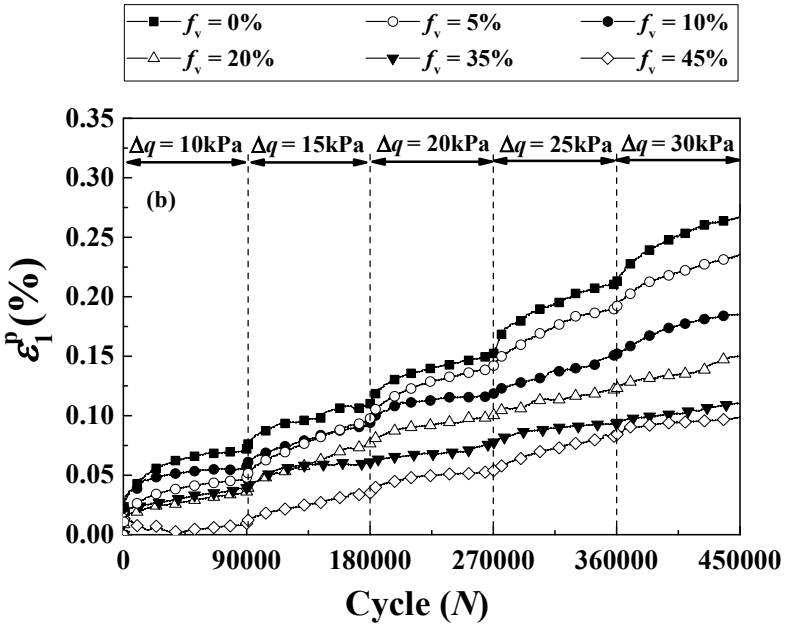
f_v = 0%
f_v = 5%
f_v = 10%
f_v = 20%
f_v = 35%
f_v = 45%
Δq = 10kPa
Δq = 15kPa
Δq = 20kPa
Δq = 25kPa
Δq = 30kPa
(b)
ε_1^p(%)
0.35
0.30
0.25
0.20
0.15
0.10
0.05
0.00
0
90000
180000
270000
360000
450000
Cycle (N)

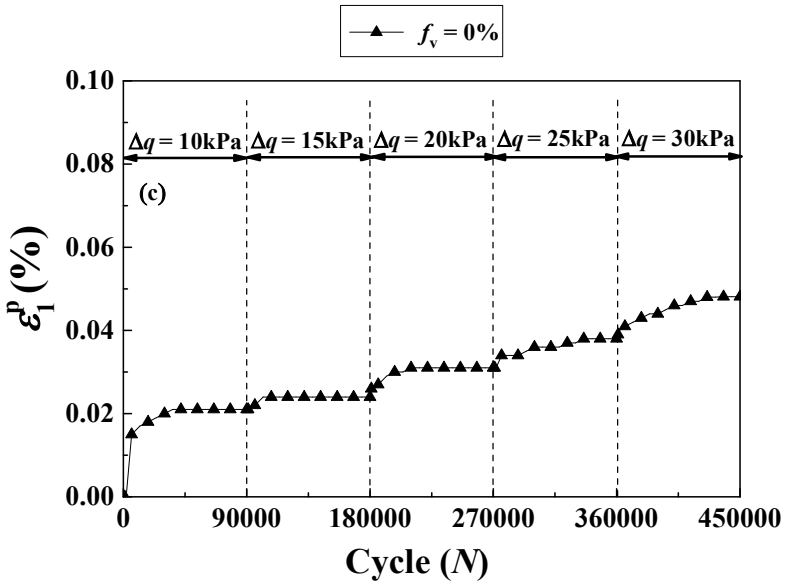

Fig. 9. Evolutions of permanent strain with number of cycles at different f_v and Δq values for various water contents: (a) w_1 = 17.6%; (b) $w_{opt\text{-}f}$ = 13.7% (after Wang et al. [4]); (c) w_2 = 10.6%

238

239 *Estimation of permanent strain*

240 Considering a multi-step loading procedure applied in this study, the loading history would
241 significantly affect the evolution of permanent strain ε_1^p with N under various water contents
242 and coarse grain contents. Thereby, the estimation approach proposed by Gidel et al. [5] was
243 adopted to eliminate such effect of loading history on permanent strain. As shown in Fig. 10,
244 the permanent strain ε_1^p evolved with N at two successive loading levels: loading level M and
245 loading level M+1. To eliminate the effect of loading level M on permanent strain at loading
246 level M+1, the increment of permanent strain $\delta\varepsilon_1^{p\,(M+1)}$ at loading level M+1 was transferred
247 to start at $\varepsilon_1^p = 0$ and N = 0, which was the starting point of permanent strain at loading level
248 M. As shown in Eq. (1), the estimated permanent strain $\varepsilon_1^{p\,(M+1)}$ at loading level M+1 without

the influence of loading history can be determined:

$$\varepsilon_1^{p\,(M+1)} = \varepsilon_1^{p\,(M)} + \delta\varepsilon_1^{p\,(M+1)} \quad (5)$$

where $\varepsilon_1^{p\,(M+1)}$ represents the estimated permanent strain at loading level M+1, $\varepsilon_1^{p\,(M)}$ represents measured permanent strain at loading level M, $\delta\varepsilon_1^{p\,(M+1)}$ represents the increment of permanent strain at loading level M+1. Note that the estimated $\varepsilon_1^{p\,(M+1)}$ at N = 90000 coincides with the measured $\varepsilon_1^{p\,(M+1)}$ at N = 180000. In addition, the slope θ of estimated $\varepsilon_1^{p\,(M+1)}$ with N after N = 90000 was kept the same as that in the last cycle of measured $\varepsilon_1^{p\,(M+1)}$, which enabled a linear increase of estimated $\varepsilon_1^{p\,(M+1)}$ with N after N = 90000 in Fig. 10.

Fig. 11 presents the evolution of the estimated ε_1^p with N at f_v = 0% and w_1 = 17.6% under various Δq values. With the increase of Δq, the estimated ε_1^p appears to grow. In addition, it can be found that the estimated ε_1^p was larger than the measure ε_1^p under the same Δq and N values (except Δq = 10 kPa). For instance, at Δq = 30 kPa and N = 450000, the estimated ε_1^p = 1.75% was much larger than the measured ε_1^p = 1.20%. This could be attributed to the effect of loading history. Different from the estimated ε_1^p under a constant Δq = 30 kPa, the measured ε_1^p experienced a series of lower stress amplitudes Δq = 10, 15, 20 and 25 kPa prior to Δq = 30 kPa, which resulted in a smaller value. Considering that a relative good accuracy for the estimated ε_1^p could be obtained at the first loading stage (e.g. N = 0 ~ 90000 in this study), as reported by Gidel et al. [5] and confirmed later by Lamas-Lopez [22] and Wang et al. [4], the estimated end-stage permanent strains ε_1^p (at N = 90000) under various Δq values were selected for further analysis.

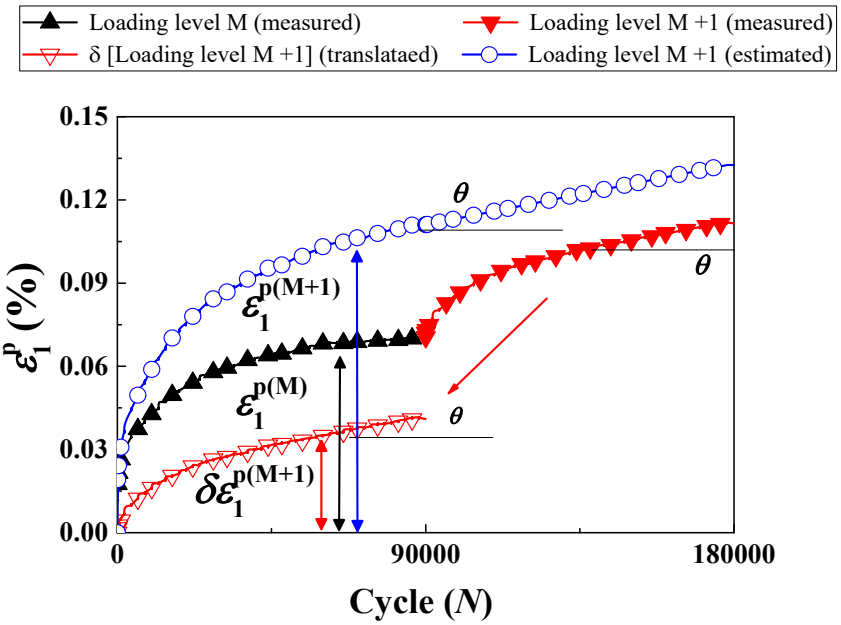

Fig. 10. Estimation method of ε_1^p proposed by Gidel et al. [5]

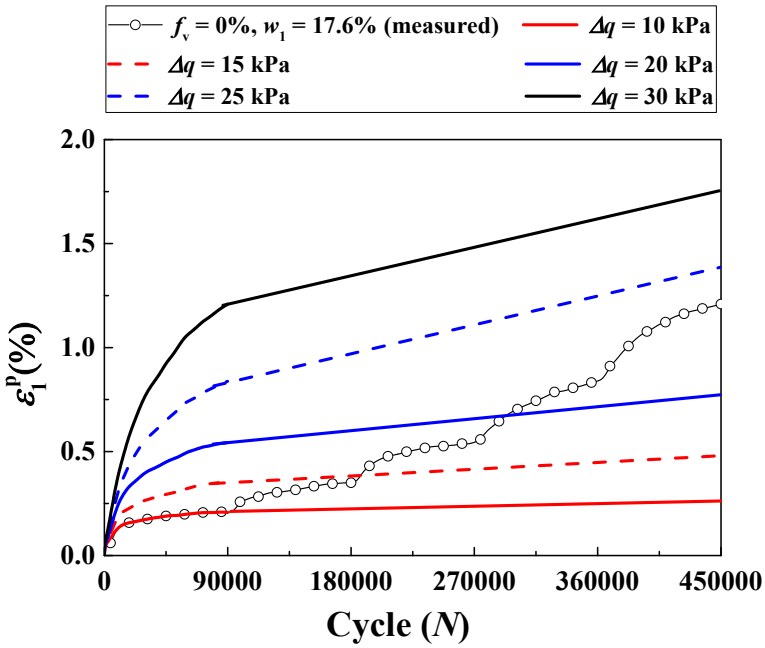

Fig. 11. Evolutions of estimated permanent strain with number of cycles at various Δq values for f_v = 0% and w_1 = 17.6%

270

Effect of water content on the variations of estimated end-stage ε_1^p with Δq

Fig. 12 shows the variations of estimated end-stage ε_1^p with Δq under different f_v values for two water contents. In the case of w_1 = 17.6% (S_r = 100%, Fig. 12 (a)), the estimated end-stage ε_1^p increased with increasing Δq for various f_v values. Under a given Δq, the ε_1^p decreased with the increase of f_v, evidencing the reinforcement effect of coarse grains. The similar observation was obtained at $w_{opt\text{-}f}$ = 13.7% (S_r = 78%) (Fig. 12 (b)). In addition, the decrease of water content from w_1 = 17.6% to $w_{opt\text{-}f}$ = 13.7% led to a decline of the estimated end-stage ε_1^p, owing to the contribution of suction.

The study of Dong et al. [12] was carried out at a constant dry density of mixture ρ_d for varying f_v values (50.3%, 55.5% and 61.4%), and therefore the fines fraction density $\rho_{d\text{-}f}$ decreased as f_v increased (Table 3). Fig. 13 shows that the estimated end-stage ε_1^p increased with Δq for the three f_v values and three w values. Under saturated conditions (w = 12%, Fig. 13 (a)), an increase of f_v led to a decrease of ε_1^p under a constant Δq, which was consistent with that observed in Fig. 12 (a). On the contrary, under unsaturated conditions (w = 6% and w = 4%, Figs. 12 (b) - (c)), an increase of f_v resulted in an increase of the estimated end-stage ε_1^p under a constant Δq, which was contradictory with the observation in Fig. 12 (b). This could be explained by the fact that the permanent strain behavior of soil mixtures was affected by both the reinforcement effect of coarse grains and the effect of suction in fines. Under saturated conditions, without the effect of suction, the reinforcement effect of f_v played a dominant role in the permanent strain behavior of mixtures. In this case, an increase of f_v induced a decrease of ε_1^p (Fig. 12 (a) and Fig. 13 (a)). By contrast, under unsaturated conditions, both the reinforcement effect of coarse grains and the effect of suction in fines

affected the permanent strain behavior. Note that the suction of fines fraction was strongly related to its $\rho_{d\text{-}f}$ under a constant water content, as evidenced by Romero et al. [26] and Gao and Sun [27] . In the present study, the fine soil was controlled at $\rho_{dmax\text{-}f}$ = 1.82 Mg/m^3 (Table 2), leading to an unchanged suction (= 739 kPa in Wang et al. [13]) at $w_{opt\text{-}f}$ = 13.7% under varying f_v values. This was supported by the findings of Su et al. [25] on the same fine/coarse soil mixture, who reported that the soil-water retention curve was only affected by the dry density of fine soil $\rho_{d\text{-}f}$, while independent of coarse grain content f_v. In this case, the reinforcement effect of f_v on the permanent strain behavior was clearly identified: an increase of f_v led to a smaller ε_1^p (Fig. 12 (b)). Conversely, in the study of Duong et al. [12] , the $\rho_{d\text{-}f}$ of fine soil declines from 1.33 Mg/m^3 to 1.17 and 0.94 Mg/m^3 with the increasing f_v values from 50.3% to 55.5% and 61.4% (Table 3), which would result in a decrease of suction within the fine fraction. In this case, the negative effect of decreasing suction prevailed on the positive reinforcement effect of increasing f_v. As a result, the ε_1^p increased with increasing f_v. (Fig. 13 (b) – (c)).

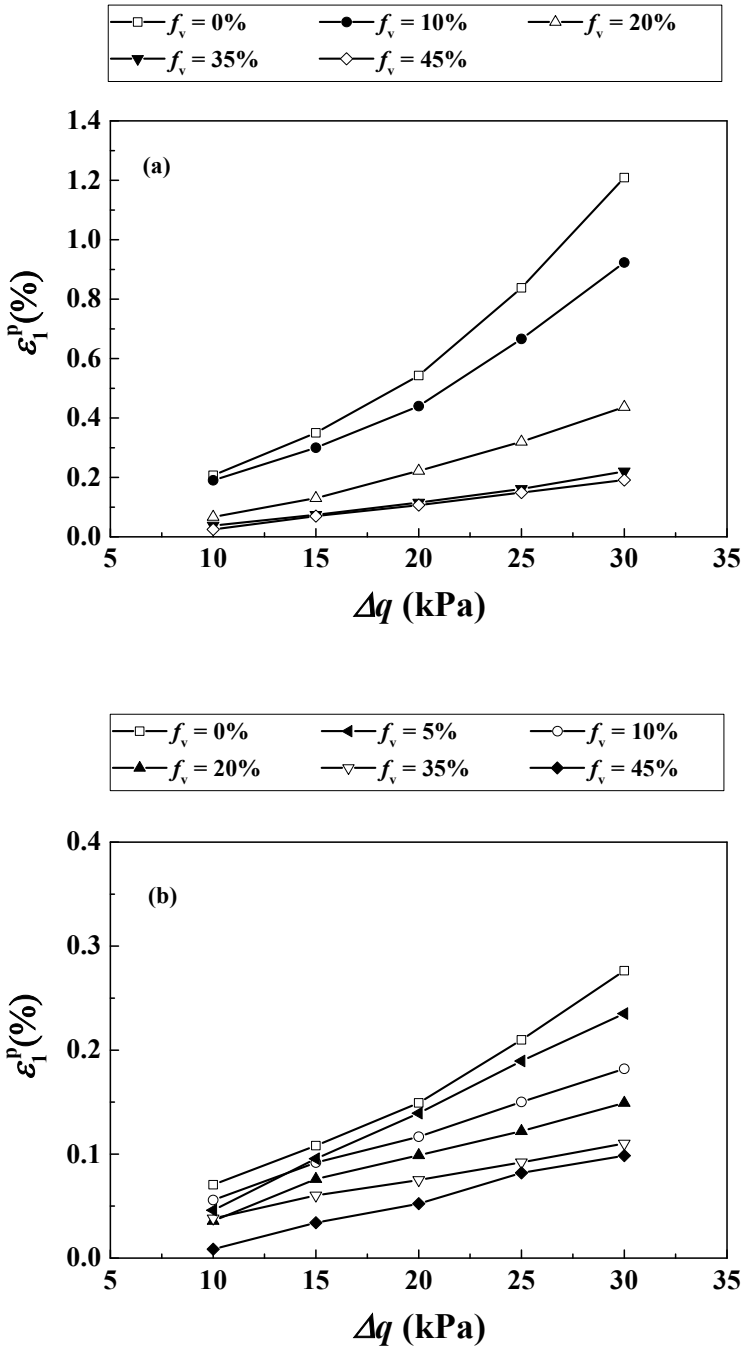

Fig. 12. Variations of estimated end-stage permanent strain with Δq at different f_v values for various water contents: (a) w_l= 17.6%; (b) $w_{opt\text{-}f}$= 13.7%

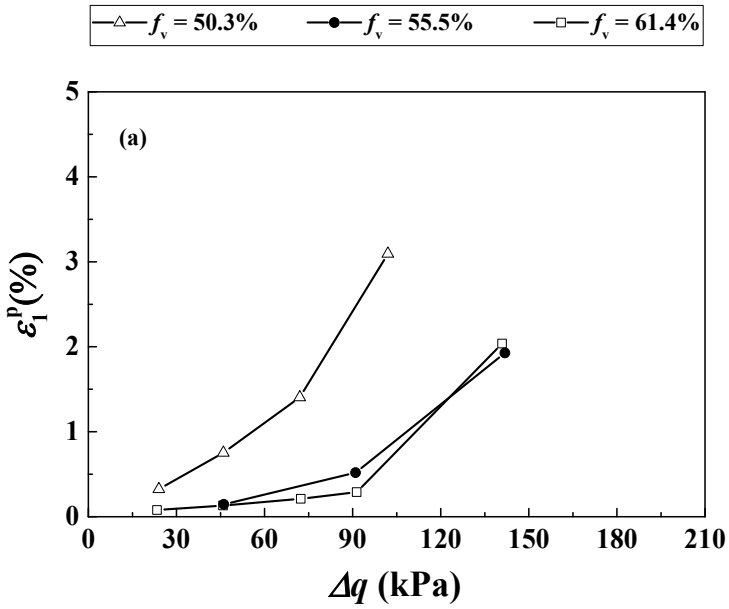
f_v = 50.3%
f_v = 55.5%
f_v = 61.4%
(a)
ε_1^p(%)
Δq (kPa)
0
1
2
3
4
5
0
30
60
90
120
150
180
210

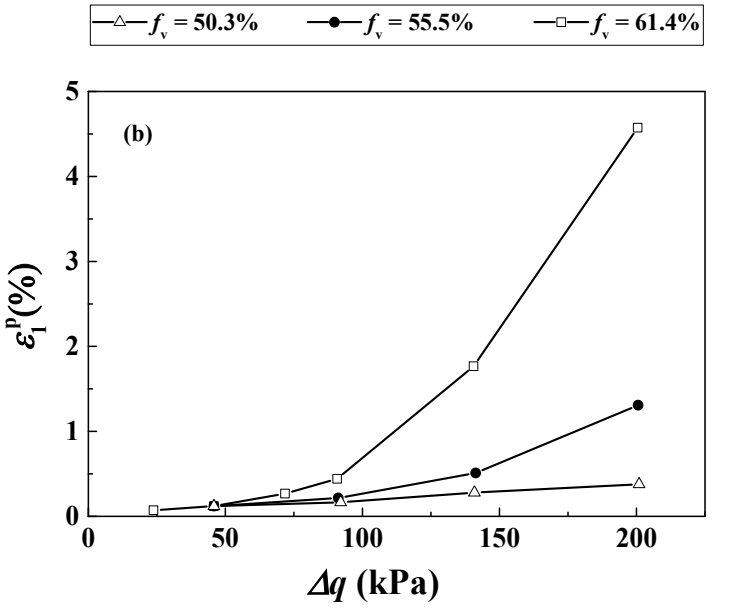
f_v = 50.3%
f_v = 55.5%
f_v = 61.4%
(b)
ε_1^p(%)
Δq (kPa)
0
1
2
3
4
5
0
50
100
150
200

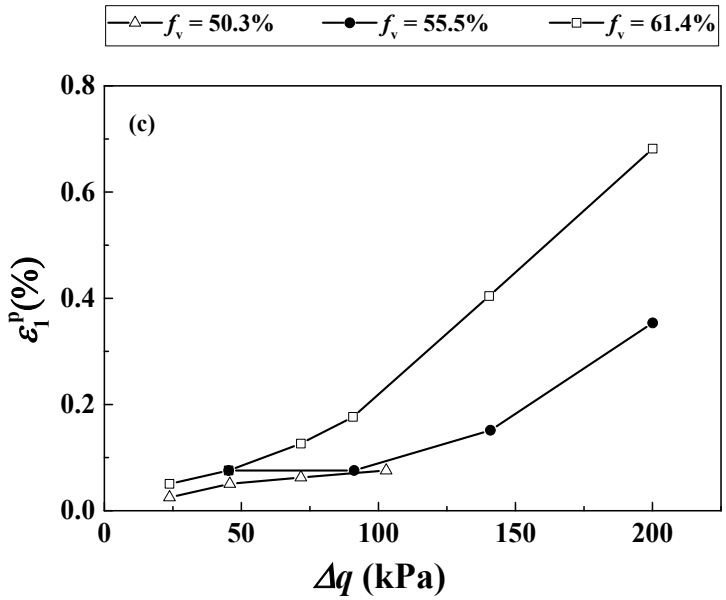

Fig. 13. Variations of estimated end-stage permanent strain with Δq at different f_v values for various water contents: (a) w = 12%; (b) w = 6%; (3) w = 4% (after Duong et al. [12])

307

Table 3. Soil properties of Duong et al. [12]

f_v (%)	w (%)				S_r (%)		ρ_d (Mg/m^3)	$\rho_{d\text{-}f}$ (Mg/m^3)
50.3	4	6	12	32	49	100	2.01	1.33
55.5	4	6	12	32	49	100		1.17
61.4	4	6	12	32	49	100		0.94

Note: w represents the water content of soil mixtures.

308

309 CONCLUSIONS

310 To investigate the effect of water content on permanent strain ε_1^p of fine/coarse soil mixtures

311 under varying coarse grain contents, a series of cyclic triaxial tests were performed. For the

312 cyclic triaxial test, a multi-step loading procedure under various stress amplitudes Δq of 10, 15,

20, 25 and 30 kPa was applied, with a number of loading cycles N = 90000 for each Δq value. Two target fines water contents w_f (w_1 = 17.6% and w_2 = 10.6%) and five coarse grain contents f_v (0%, 10%, 20%, 35% and 45%) were considered. The estimation approach of ε_1^p proposed by Gidel et al. [5] was adopted to eliminate the effect of loading history on ε_1^p. Through the comparison of the present study and the study of Duong et al. [12], the effects of water content and coarse grain content on the permanent strain behavior of fine/coarse soil mixtures were clarified. The following conclusions to be drawn:

A decrease of water content led to a decrease of permanent strain ε_1^p, due to the contribution of suction. An increase of f_v gave rise to a decrease of ε_1^p, owing to the reinforcement effect of f_v. The comparison of present study and the study of Duong et al. [12] indicated a significant effect of sample preparation approach on the permanent strain behavior of soil mixtures. In the present study, a constant $\rho_{d\text{-}f}$ of fine soil fraction was maintained, leading to an unchanged suction of soil mixtures with varying f_v values. In this case, the reinforcement effect of f_v on the permanent strain behavior was clearly identified: an increase of f_v led to a decrease of ε_1^p. Conversely, in the study of Duong et al. [12], with a global dry density kept constant, an increase of f_v led to a decrease of the dry density of fines $\rho_{d\text{-}f}$ and consequently a decrease of suction. In that case, when the negative effect of decreasing suction prevailed on the positive reinforcement effect of increasing f_v, the ε_1^p increased with the increase of f_v.

ACKNOWLEDGEMENTS

This work was supported by the China Scholarship Council (CSC) and Ecole des Ponts ParisTech.

REFERENCES

[1] Trinh, V. N. (2011). Comportement hydromécanique des matériaux constitutifs de plateformes ferroviaires anciennes. PhD Thesis, Ecole Nationale des Ponts et Chaussées, Université Paris-Est.

[2] Cui, Y.J., Duong, T.V., Tang, A.M., Dupla, J.C., Calon, N. and Robinet, A., (2013). Investigation of the hydro-mechanical behaviour of fouled ballast. Journal of Zhejiang University Science A, 14(4), pp.244-255.

[3] Song, Y., & Ooi, P. S. (2010). Interpretation of shakedown limit from multistage permanent deformation tests. Transportation research record, 2167(1), 72-82.

[4] Wang, H.L., Cui, Y.J., Lamas-Lopez, F., Dupla, J.C., Canou, J., Calon, N., Saussine, G., Aimedieu, P. and Chen, R.P., (2018). Permanent deformation of track-bed materials at various inclusion contents under large number of loading cycles. *Journal of Geotechnical and Geoenvironmental Engineering*, *144*(8), p.04018044.

[5] Gidel, G., Hornych, P., Breysse, D., & Denis, A. (2001). A new approach for investigating the permanent deformation behaviour of unbound granular material using the repeated loading triaxial apparatus. Bulletin des laboratoires des Ponts et Chaussées, (233).

[6] Werkmeister, S., Dawson, A. R., & Wellner, F. (2001). Permanent deformation behavior of granular materials and the shakedown concept. Transportation Research Record, 1757(1), 75-81.

[7] Nie, R., Li, Y., Leng, W., Mei, H., Dong, J., & Chen, X. (2020). Deformation characteristics of fine-grained soil under cyclic loading with intermittence. *Acta Geotechnica*, 1-14..

[8] Trinh, V.N., Tang, A.M., Cui, Y.J., Dupla, J.C., Canou, J., Calon, N., Lambert, L., Robinet, A. and Schoen, O., (2012). Mechanical characterisation of the fouled ballast in ancient railway track substructure by large-scale triaxial tests. *Soils and foundations*, *52*(3), pp.511-523.

[9] Jing, P. (2017). Experimental study and modelling of the elastoplastic behaviour of unbound granular materials under large number of cyclic loadings at various initial hydric states (Doctoral dissertation).

[10] Wan, Z., Bian, X., Li, S., Chen, Y., & Cui, Y. (2020). Remediation of mud pumping in ballastless high-speed railway using polyurethane chemical injection. Construction and Building Materials, 259, 120401.

[11] Gu, C., Zhan, Y., Wang, J., Cai, Y., Cao, Z., & Zhang, Q. (2020). Resilient and permanent deformation of unsaturated unbound granular materials under cyclic loading by the large-scale triaxial tests. *Acta Geotechnica*, *15*(12), 3343-3356.

[12] Duong, T.V., Tang, A.M., Cui, Y.J., Trinh, V.N., Dupla, J.C., Calon, N., Canou, J. and Robinet, A., (2013). Effects of fines and water contents on the mechanical behavior of

interlayer soil in ancient railway sub-structure. *Soils and foundations*, *53*(6), pp.868-878.

[13] Wang, H.L., Cui, Y.J., Lamas-Lopez, F., Calon, N., Saussine, G., Dupla, J.C., Canou, J., Aimedieu, P. and Chen, R.P., (2018). Investigation on the mechanical behavior of track-bed materials at various contents of coarse grains. *Construction and Building Materials*, *164*, pp.228-237.

[14] Qi, S., Cui, Y.J., Chen, R.P., Wang, H.L., Lamas-Lopez, F., Aimedieu, P., Dupla, J.C., Canou, J. and Saussine, G., (2020). Influence of grain size distribution of inclusions on the mechanical behaviours of track-bed materials. Géotechnique, 70(3), pp.238-247.

[15] Su, Y., Cui, Y. J., Dupla, J. C., & Canou, J. (2020). Investigation of the effect of water content on the mechanical behavior of track-bed materials under various coarse grain contents. Construction and Building Materials, 263, 120206.

[16] Su, Y., Cui, Y. J., Dupla, J. C., Canou, J., & Qi, S. (2020). A fatigue model for track-bed materials with consideration of the effect of coarse grain content. Transportation Geotechnics, 23, 100353.

[17] Su, Y., Cui, Y. J., Dupla, J. C., & Canou, J. (2021). Effect of water content on resilient modulus and damping ratio of fine/coarse soil mixtures with varying coarse grain contents. Transportation Geotechnics, 26, 100452.

[18] Qi, S., Cui, Y.J., Dupla, J.C., Chen, R.P., Wang, H.L., Su, Y., Lamas-Lopez, F. and Canou, J., (2020b). Investigation of the parallel gradation method based on the response of track-bed materials under cyclic loadings. Transportation Geotechnics, p.100360.

398 [19] Su, Y., Cui, Y. J., Dupla, J. C., Canou, J., & Qi, S. (2021). Developing a Sample
399 Preparation Approach to Study the Mechanical Behavior of Unsaturated Fine/Coarse
400 Soil Mixture. Geotechnical Testing Journal, 44(4).
401 [20] Wang, H. L., Cui, Y. J., Lamas-Lopez, F., Dupla, J. C., Canou, J., Calon, N., ... &
402 Chen, R. P. (2017). Effects of inclusion contents on resilient modulus and damping
403 ratio of unsaturated track-bed materials. Canadian Geotechnical Journal, 54(12), 1672-
404 1681.
405 [21] Duong, T.V., Cui, Y.J., Tang, A.M., Dupla, J.C., Canou, J., Calon, N. and Robinet, A.,
406 (2016). Effects of water and fines contents on the resilient modulus of the interlayer
407 soil of railway substructure. *Acta Geotechnica*, *11*(1), pp.51-59.
408 [22] Lamas-lopez, F. (2016). Field and laboratory investigation on the dynamic behavior of
409 conventional railway track-bed materials in the context of traffic upgrade. PhD Thesis,
410 Ecole Nationale des Ponts et Chaussées, Université Paris-Est.
411 [23] Duong, T. V., Cui, Y. J., Tang, A. M., Dupla, J. C., & Calon, N. (2014). Effect of fine
412 particles on the hydraulic behavior of interlayer soil in railway substructure. Canadian
413 geotechnical journal, 51(7), 735-746.
414 [24] Jing, P., Nowamooz, H., & Chazallon, C. (2018). Permanent deformation behaviour of
415 a granular material used in low-traffic pavements. Road Materials and Pavement
416 Design, 19(2), 289-314.
417 [25] Su, Y., Cui, Y. J., Dupla, J. C., & Canou, J. (2021). Soil-water retention behaviour of
418 fine/coarse soil mixture with varying coarse grain contents and fine soil dry densities.
419 Canadian Geotechnical Journal, (ja).

[26] Romero, E., Gens, A., & Lloret, A. (1999). Water permeability, water retention and microstructure of unsaturated compacted Boom clay. Engineering Geology, 54(1-2), 117-127.

[27] Gao, Y., Sun, DA. (2017). Soil-water retention behavior of compacted soil with different densities over a wide suction range and its prediction. Computers and Geotechnics, 91, 17-26.

NOTATIONS

ε_1	axial strain
ε_1^r	resilient strain
ε_1^p	permanent strain
$\varepsilon_1^{p\,(M)}$	measured permanent strain at loading level M
$\varepsilon_1^{p\,(M+1)}$	estimated permanent strain at loading level M+1
$\delta\varepsilon_1^{p\,(M+1)}$	increment of permanent strain at loading level M+1
f_{v}	volumetric coarse grain content
$f_{\mathrm{v\text{-}cha}}$	characteristic volumetric coarse grain content
N	number of loading cycles
ρ_{d}	dry density of sample
$\rho_{\mathrm{d\text{-}f}}$	dry density of fine soil
$\rho_{\mathrm{dmax\text{-}f}}$	maximum dry density of fine soil
q	deviator stress

q_{max}	maximum deviator stress
q_{min}	minimum deviator stress
Δq	deviator stress amplitude
Δp	mean stress amplitude
S_r	degree of saturation
$w_{opt\text{-}f}$	optimum water content of fine soil
w_f	water content of fine soil
σ_3	confining pressure
θ	increasing slope of permanent strain with loading cycles at the end of loading cycles for a given stress amplitude

429 LIST OF TABLES

430

LIST OF FIGURES

431